INTERNATIONAL SOCIETY FOR SOIL MECHANICS AND GEOTECHNICAL ENGINEERING

A numerical investigation into the transverse permeability of fibrous geomaterials

Une étude numérique sur la perméabilité transversale des géomatériaux fibreux

Thanh Trung Nguyen
Centre for Geomechanics and Railway Engineering, PhD Student, University of Wollongong, Australia, ttn323@uowmail.edu.au

Buddhima Indraratna
Faculty of Engineering and Information Sciences, Distinguished Professor of Civil Engineering, University of Wollongong, Australia.

Cholachat Rujikiatkamjorn
Faculty of Engineering and Information Sciences, Associate Professor of Civil Engineering, University of Wollongong, Australia.

ABSTRACT: Fibrous geomaterials are widely used in geo-engineering practices for stabilisation, filtration and drainage. Most applications rely on their exceptional hydraulic conductivity despite the current paucity of numerical methods which can simultaneously capture the behaviour of fibre and fluid. In this paper, a coupling numerical approach is proposed where fibres are modelled by Discrete Element Method (DEM) and fluid is simulated by Finite Volume Method (FVM). The Parallel Bond Model incorporated in DEM will reasonably capture the linear stress-strain behaviour of natural fibres such as jute, but unlike previous studies where the fibres are either pre-formed and have an unchanged geometry, the coupling technique provides a good agreement in predicting the hydraulic behaviour of fibrous porous media. The motion of fibres due to fluid flow is also analysed.

RÉSUMÉ: Les géomatériaux fibreux sont largement utilisés dans les pratiques de géo-ingénierie par exemple la stabilisation, la filtration et le drainage. La plupart des applications de matériaux fibreux reposent sur leur conductivité hydraulique exceptionnelle alors qu'il existe une limitation de méthode numériques qui sont incapable de capturer des comportements de fibre et de fluide simultanément. Dans cet article, une approche numérique de couplage de les fibres et fluide est présenté. Les fibres sont modélisées par la méthode des éléments discrets (DEM) et le fluide est simulée par la méthode de volume fini (Finite Volume Method). Le modèle de liaison parallèle incorporé dans DEM capturer raisonnablement le comportement linéaire contrainte-déformation de fibres naturelles, par exemplele jute. En comparaison com études antérieures que utilisés la géométrie préformée et non modifiée des fibres, la technique de couplage permet d'obtenir un bon accord pour prédire le comportement hydraulique des milieux poreux fibreux. Le mouvement des fibres dû à l'écoulement du fluide est également analysé.

KEYWORDS: CFD-DEM coupling, natural fibres, geomaterials, permeability, hydraulic behavior

1 INTRODUCTION

Natural fibres such as jute and coir have been used extensively in geoengineering practices for many years, particularly for filtration and drainage. The key mechanism here is the hydraulic behaviour of fluid as it flows through a fibrous porous system, a mechanism that has been studied over the preceding years (Palmeira et al. 2005; Asha and Mandal 2012). While the common methods are experimental and analytical due to their simplicity, they are limited when a comprehensive solution is needed in design, which is why the flexible and extremely accurate numerical approach has received more attention in recent decades. Previous works which used the Finite Element Method (FEM) (Yazdchi et al. 2011) only considered fibrous media with a constant geometry, the mutual interaction between the fluid and solid phases was ignored, and thus the predictions could deviate. This is why computational scheme which captures the dynamic behaviour of fluid-fibre media is essential.

Nguyen and Indraratna (2016b) used the Discrete Element Method (DEM) coupled with Computational Fluid Dynamics (CFD) to investigate the longitudinal permeability of the parallel arrangement of fibres. This study indicates there is a good agreement between the proposed method and previous studies where experimental and analytical approaches are used

to estimate the permeability of fibrous media in a steady state. To verify this solution relative to natural fibre drains, Nguyen and Indraratna (2016a) used microanalysis to capture the porous characteristics of a drain and then use them for the numerical work. These studies have provided a launching pad from which to broaden the application of fluid-particle coupling scheme to model the hydraulic behavior of geomaterials.

This paper explains an application of the CFD-DEM coupling approach to simulate a transverse flow through parallel fibres, where the Parallel Bond Model incorporated in DEM is used to model fibres and the fluid is captured by the Finite Volume Method (FVM). The permeability of a fibre bundle under a perpendicular flow is estimated and then compared to those obtained in previous studies. In this investigation, DEM codes are implemented on an open source software named LIGGGHTS (Kloss and Goniva 2010) while the FVM is incorporated into the free code OpenFOAM (2014); the two codes can then interact using the platform CFDEM (Goniva et al. 2010).

2 THEORETICAL BACKGROUNDS

2.1 Fundamentals of the discrete element method

The Discrete Element Method (DEM) has increasingly been used to simulate the behaviour of ganular materials such as sand and rock (Bertrand et al. 2005; Zeghal and El Shamy 2008; Ngo

et al. 2014). In this method the motion of a particle is governed by following equations:

$$m_i \frac{dU_{p,i}}{dt} = \sum_{j=1}^{n_i} F_{c,ij} + F_{f,i} + F_{g,i} \qquad (1)$$

$$I_i \frac{\omega_{p,i}}{dt} = \sum_{j=1}^{n_i} M_{c,ij} \qquad (2)$$

where the subscripts i and j represent particles i and j, respectively; m_i is the mass; $U_{p,i}$ and $\omega_{p,i}$ are the translational and angular velocities, respectively; I_i is referred to as the moment of inertia: $F_{c,ij}$ and $M_{c,ij}$ are the contact force and torque acting on particle i by particle j (or walls), while n_i is the number of total contacts. $F_{g,i}$ is the gravitational force, and $F_{f,i}$ is the total fluid-particle interaction force.

2.2 Fluid flow behaviour

The continuum and conservation of an incompressible fluid can be described by the locally averaged Navier-Stokes equations as follows:

$$\frac{\partial n}{\partial t} + \nabla.(nU_f) = 0 \qquad (3)$$

$$\frac{\partial(\rho_f nU_f)}{\partial t} + \nabla.(\rho_f nU_f U_f) = \\ = -n\nabla p - f_p + \nabla.(n\tau) + n\rho_f g \qquad (4)$$

In the above, n is the porosity of a certain fluid cell and is defined as the ratio of the void volume in a cell to its total volume V_c: $n = V_v/V_c = 1 - V_p/V_c$ where V_v, V_p are the volume of the void and particles occupied in such a cell, respectively. Note here that the fluid domain is divided into a finite number of cells where fluid parameters such as the velocity, pressure, porosity are governed locally in each cell. τ is the viscous stress tensor and ρ_f is the fluid density; f_p is the mean volumetric particle-fluid interaction force representing the effect that the solid phase has on the fluid within the cell. By considering that the fluid cell β contains n_p particles, the f_p of cell β can be estimated by Eq. 5 as follows:

$$f_{p,\beta} = \sum_{i=1}^{n_{p,\beta}} \varpi_{i\beta} \left(\frac{F_{p,i}}{V_{c,\beta}} \right) \qquad (5)$$

where $F_{p,i}$ is the total force acting on particle i; $V_{c,\beta}$ is the volume of the fluid cell β. The factor $\varpi_{i\beta}$ representing the volumetric portion of particle i residing in cell β is estimated as the ratio of the exact volumetric portion of particle i in cell β to the total volume of cell β.

2.3 Fluid particle interaction forces

Fluid flow can cause a number of forces to act on particles, including: (*i*) the drag force; (*ii*) the pressure acceleration force; (*iii*) the buoyancy force; (*iv*) the viscous force; and (*v*) is other unsteady forces. In this study the unsteady forces are ignored because they are usually insignificant compared to the drag and pressure acceleration forces (Zhu et al. 2007; Zhou et al. 2010).

The drag force using De Felice's model (Zhou et al. 2010) is as follows:

$$F_{d,i} = \frac{1}{8} C_d \rho_f \pi D_{p,i}^2 n_\beta^2 (U_{f,\beta} - U_{p,i}) |U_{f,\beta} - U_{p,i}| n_\beta^{-\chi} \qquad (6)$$

where $D_{p,i}$ is the diameter; $U_{f,\beta}$ and $U_{p,i}$ are the velocity of fluid in cell β and particle i, respectively. C_d is the fluid-particle drag coefficient that is computed by:

$$C_d = \left(0.63 + \frac{4.8}{\sqrt{Re_{p,i}}} \right)^2 \qquad (7)$$

In the above $Re_{p,i}$ is the particle Reynolds number which is estimated as follows:

$$Re_{p,i} = \frac{n_\beta \rho_f D_{p,i} |U_{f,\beta} - U_{p,i}|}{\mu_f} \qquad (8)$$

The porosity function $n_\beta^{-\chi}$ represents the influence of other particles in cell β in relation to the power factor χ which is calculated by:

$$\chi = 3.7 - 0.65 \exp \left[-\frac{(1.5 - \log_{10} Re_{p,i})^2}{2} \right] \qquad (9)$$

The pressure acceleration force accounting for a difference in hydraulic pressure through the flow is represented as follows:

$$F_{\nabla p,i} = -(\nabla p) V_{p,i} \qquad (10)$$

The buoyancy force is computed by:

$$F_{b,i} = -\rho_f g V_{p,i} \qquad (11)$$

The viscous stress is generated when there is a variation in fluid velocity over a region, which results in the viscous force acting on particles as follows:

$$F_{\nabla.\tau,i} = (\nabla.\tau) V_{p,i} \qquad (12)$$

Note that for a homogeneous medium, the fluid velocity is uniform over different cells, making this force insignificant.

The total fluid-particle interaction force $F_{f,i}$ therefore includes:

$$F_{f,i} = F_{d,i} + F_{\nabla p,i} + F_{b,i} + F_{\nabla.\tau,i} \qquad (13)$$

3 MODELLING TRANSVERSE FLOW THROUGH FIBRES

3.1 Fibre modelling

Fibre is a continuum which can be divided into a number of discrete elements with bonding. This technique has been used with reasonable success by Nguyen and Indraratna (2016a, b) when simulating natural jute and coir fibres. They adopted the original Parallel Bond Model (PBM) to capture the linear stress-strain relationship (e.g., jute, bamboo) and then proposed a modified version to describe the non-linear behaviour of coir fibres. In this paper, the original PBM proposed by Potyondy and Cundall (2004) is used for the sake of simplicity.

Figure. 1 represents the linear tensile behaviour of jute fibre simulated by the PBM incorporated in DEM, which matches the experimental result very well. The fibre is broken when the stress reaches its tensile strength. Figure 1b shows a tensile test carried out on a bundle of jute fibre. Jute has an almost linear

stress-strain relationship and a brittle fracture that can reasonably be captured by PBM. The bond stiffness k_{bn} of 1.85×10^{11} N/m and k_{bs} of 5.0×10^{11} N/m are a reasonable was of describing the tensile and bending behaviour of jute.
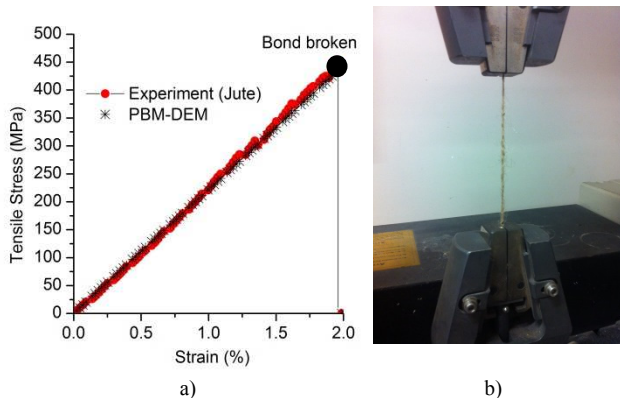

Figure 1. Tension test: a) DEM and experimental results; b) Experiment

3.2 Modelling fluid flow

A velocity controlled model where the fluid velocity is manipulated at the input and set as zero at the output of the domain is used. The fluid domain is discretised into a finite number of cells where fluid variables, i.e., the velocity, pressure and porosity are governed locally by Eq. 3 and 4. The size of fluid cell is larger than the maximum diameter of DEM particles. The pressure drop as fluid flowing horizontally through fibre bundle is obtained from CFD domain with respect to the fibre motion captured by DEM, for calculating the permeability as follows:

$$K = -\frac{U_{f,s}\mu_f}{\nabla p} \qquad (14)$$

where K is the permeability; Δp is the pressure drop when fluid travels over a length L; $U_{f,s}$ is the superficial velocity and μ_f is the dynamic viscosity of the fluid.
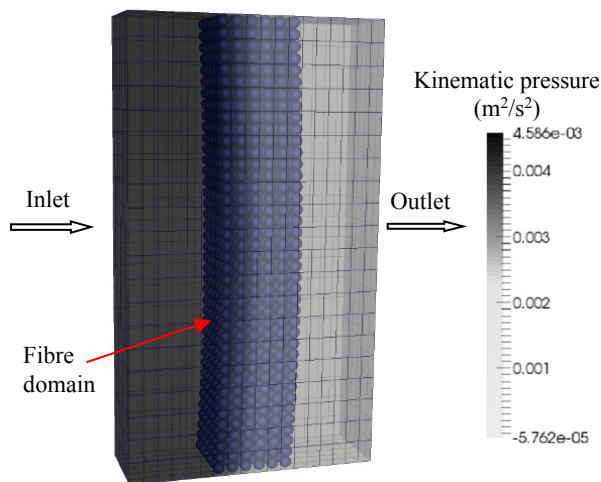

Figure 2. Pressure drop as transverse flow through fibre bundle

Figure 2 shows how the fluid domain can be discretised and the contour of the pressure drop can be obtained as fluid flowing through a fibre medium. In this investigation, the fibre domain is 5 mm thick and the porosity is 0.65. The fibres are arranged in parallel and are assumed to have a uniform diameter of 80 μm. The fluid pressure under an input velocity

0.01 m/s decreases from 4.5 Pa (kinematic pressure, $p/\rho_f = 4.5 \times 10^{-3}$ m²/s²) to zero at the outlet as Figure 2 shows.

4 RESULTS AND DISCUSSION

4.1 Transverse permeability of fibre bundle

To compare with previous studies which considered fibres to be completely unchanged when fluid is flowing, two ends of the fibres are fixed to minimise the influence of their deformation on the hydraulic behaviour. Figure 3 represents the variation of transverse permeability of parallel fibres over different magnitudes of porosity, as obtained by the CFD-DEM coupling technique. In the medium range of fibre fraction (i.e., $0.45 < n < 0.8$), the dimensionless permeability varies from 2.5×10^{-3} to almost 1.0×10^{-1}. The slope of the reduction curve becomes steeper when the fibre bundle becomes either denser (i.e., $n < 0.38$) or looser (i.e., $n > 0.85$).
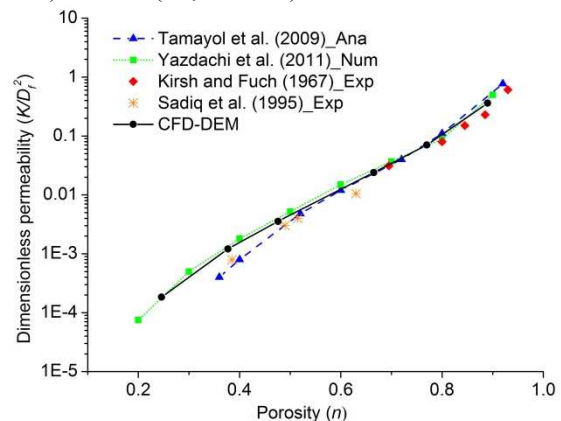

Figure 3. Variation of transverse permeability over porosity

Figure 3 shows a comparison between the permeability obtained by a CFD-DEM coupling and those gained in previous studies, which include: (i) an analytical approach by Tamayol and Bahrami (2009) which considers the parabolic distribution of fluid velocity; (ii) Yazdchi et al. (2011) use of the Finite Element Method (FEM) to solve Navier-Stokes equations; and (iii) an experimental approach by Kirsch and Fuchs (1967) and Sadiq et al. (1995). The approach proposed to solve the locally averaged Navier-Stokes equations by the finite volume method (FVM) results in almost the same hydraulic behaviour as that obtained by the FEM. Note that while conventional FEM generates pre-formed solid fibres and maintains them unchanged over time, the CFD-DEM coupling can capture the variation of fibres and fluid behaviour by considering the fluid-solid interaction.

Unlike the experimental and analytical works, the result gained in this study agrees when $n > 0.5$ but it deviates as $n < 0.45$. For example, at $n = 0.4$ the dimensionless permeability by Saquid et al. (1995) and Tamayol and Bahrami (2009) is approximately 9×10^{-4} and 8.2×10^{-4} respectively, but the coupling technique has a higher value, i.e., 1.7×10^{-3}.

4.2 Fibre motion under fluid flow

To investigate how the fluid-fibre interaction forces affect the arrangement of fibre, one end is fixed and other end is allowed to move, and a flow perpendicular to fibres under an input velocity of 0.01 m/s is generated. Note that in this model, a slip boundary is adopted which results in a uniform distribution of fluid velocity along the fibres, and the fibres bend under fluid-interaction forces inserted on them, as Figure 4 shows. The velocity of fibre particles decreases over the length of the fibres,

which has a static condition at the bottom ends. Note that apart from the fluid-particle interaction forces summarised in Eq 13, the bond stiffness (i.e., k_{bn} and k_{bs}) which affects the tensile and bending behaviour of fibres plays an important role in rearranging tdhe fibres under fluid flowing.
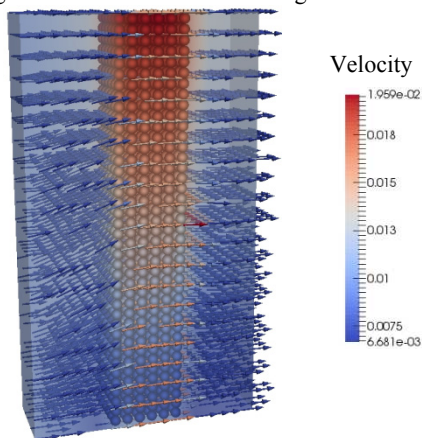

Figure 4. Fibres moving under a perpendicular flow

The horizontal displacement of particles at different positions in the fibres over a time increment is shown in Figure 5. The higher the particles are from the fixed bottom end, the larger the displacement. In fact the fibre tip (i.e., 3.2 mm high) is displaced by almost 0.64 mm after 4×10^6 time steps, while the bottom is zero because it is restrained. This deformation is reasonable with respect to beam theory when a beam is subjected to a load distributed along it.
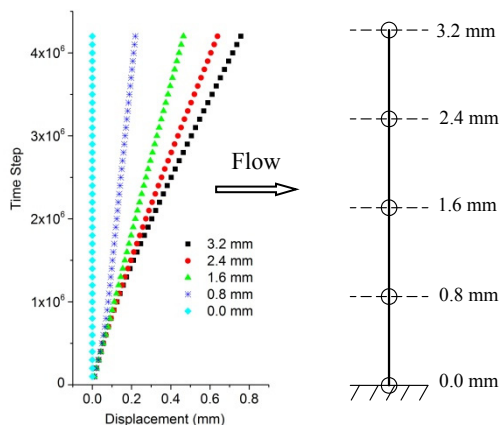

Figure 5. Horizontal displacements induced by transverse flow

5 CONCLUSION

This paper has proposed a numerical approach where solid fibres are simulated by DEM in parallel to fluid described by CFD to model a transverse flow through fibrous media. For a steady state where two ends of the fibres are restrained, the transverse permeability which resulted from the fluid-particle coupling agrees with those obtained from previous studies where completely immobilised fibres were used. This current study can simulate all the previous predictions, particularly the experimental, numerical, and analytical works when $n > 0.5$, but the deviation became significant as $n < 0.45$. This result was almost identical to when FEM was used to solve the Navier-Stokes equations implemented by Yazdchi et al. (2011) for the whole range of porosity. This study also represented a reasonable deformation of fibre under horizontal fluid flow. The displacement of fibre particles decreased from 0.64 mm to zero over the length of the fibres under fluid-particle interaction forces. This study indicates a certain success at capturing the discrete and continuum behaviours of a fluid-fibre system in geoengineering.

7 REFERENCES

Asha, B.S. and Mandal, J.N. 2012. Absorption and discharge capacity tests on natural prefabricated vertical drains. Geosynthetics International, 19: 263-271.

Bertrand, F., Leclaire, L.A. and Levecque, G. 2005. DEM-based models for the mixing of granular materials. Chemical Engineering Science, 60(8–9): 2517-2531. doi: http://j.doi.org/10.1016/j.ces.2004.11.048.

Goniva, C., Kloss, C., Hager, A. and Pirker, S. 2010. An open source CFD-DEM perspectives. In Proceeding of the 5th OpenFOAM Workshop, Gothenburg, Sweden.

Kirsch, A.A. and Fuchs, N.A. 1967. Studies on Fibrous Aerosol Filters—II. Pressure Drops in Systems of Parallel Cylinders. Annals of Occupational Hygiene, 10(1): 23-30. doi: 10.1093/annhyg/10.1.23.

Kloss, C. and Goniva, C. 2010. LIGGGHTS: a new open source discrete element simulation software. In Proceeding of the 5th International Conference on Discrete Element Methods, London, UK.

Ngo, N.T., Indraratna, B. and Rujikiatkamjorn, C. 2014. DEM simulation of the behaviour of geogrid stabilised ballast fouled with coal. Computers and Geotechnics, 55: 224-231. doi: http://dx.doi.org/10.1016/j.compgeo.2013.09.008.

Nguyen, T.T. and Indraratna, B. 2016a. Experimental and numerical investigations into hydraulic behaviour of coir fibre drain. Canadian Geotechnical Journal. doi: http://www.nrcresearchpress.com/doi/10.1139/cgj-2016-0182#.V85Bofl97IU.

Nguyen, T.T. and Indraratna, B. 2016b. Hydraulic behaviour of parallel fibres under longitudinal flow: a numerical treatment. Canadian Geotechnical Journal, 53(7): 1081-1092.

OpenFOAM. 2014. OpenFOAM user guide, Version 2.3.0.

Palmeira, E.M., Gardoni, M.G. and Luz, D.W.B.d. 2005. Soil–geotextile filter interaction under high stress levels in the gradient ratio test. Geosynthetics International, 12(4): 162-175. doi: doi:10.1680/gein.2005.12.4.162.

Potyondy, D.O. and Cundall, P.A. 2004. A bonded-particle model for rock. International Journal of Rock Mechanics and Mining Sciences, 41(8): 1329-1364.

Sadiq, T.A.K., Advani, S.G. and Parnas, R.S. 1995. Experimental investigation of transverse flow through aligned cylinders. International Journal of Multiphase Flow, 21(5): 755-774. doi: http://dx.doi.org/10.1016/0301-9322(95)00026-T.

Tamayol, A. and Bahrami, M. 2009. Analytical determination of viscous permeability of fibrous porous media. International Journal of Heat and Mass Transfer, 52(9–10): 2407-2414.

Yazdchi, K., Srivastava, S. and Luding, S. 2011. On the validity of the carman-kozeny equation in random fibrous media. In ECCOMAS Conference on Particle-based Methods II - Fundamentals and Applications, Barcelona, Spain. pp. 264-273.

Zeghal, M. and El Shamy, U. 2008. Liquefaction of saturated loose and cemented granular soils. Powder Technology, 184(2): 254-265. doi: http://dx.doi.org/10.1016/j.powtec.2007.11.032.

Zhou, Z.Y., Kuang, S.B., Chu, K.W. and Yu, A.B. 2010. Discrete particle simulation of particle–fluid flow: model formulations and their applicability. Journal of Fluid Mechanics, 661: 482-510. doi: doi:10.1017/S002211201000306X.

Zhu, H.P., Zhou, Z.Y., Yang, R.Y. and Yu, A.B. 2007. Discrete particle simulation of particulate systems: theoretical developments. Chemical Engineering Science, 62(13): 3378-3396